

BIOPHOTONICS

DOI: 10.1070/QEL16185

Effects of haemodilution on the optical properties of blood during coagulation studied by optical coherence tomography

B. Liu, Y. Liu, H. Wei, X. Yang, G. Wu, Z. Guo, H. Yang, Y. He, S. Xie

Abstract. **We report an investigation of the effects of blood dilution with hypertonic (7.5%) and normal (0.9%) saline on its optical properties during coagulation *in vitro* using optical coherence tomography. The light penetration depth and attenuation coefficient are obtained from the dependences of reflectance on the depth. Normal whole blood has served as the control group. The average coagulation time is equal to 420 ± 16, 418 ± 16 and 358 ± 14 s with blood volume replacement of 2%, 11%, and 20% by 0.9% normal saline, respectively. With 2%, 11% and 20% blood volume replacement with 7.5% hypertonic saline, the average coagulation time is 422 ± 17, 1160 ± 45 and 1730 ± 69 s, respectively. For normal whole blood, the average coagulation time amounts to 425 ± 19 s. it is shown that dilution with normal saline has a procoagulant effect when it replaces 20% of blood volume, and hypertonic saline has an anticoagulant effect if it replaces 11% or more of blood volume. It is concluded that optical coherence tomography is a potential technique to quantify and monitor the liquid–gel transition during the coagulation process of blood diluted by normal and hypertonic saline.**

Keywords: *optical coherence tomography, blood, coagulation, haemodilution, optical properties.*

1. Introduction

Blood coagulation is a host defense mechanism that assists in maintaining the integrity of the closed, high-pressure mammalian circulatory system when a vein or artery is pierced or broken [1]. As we know, the wounds which have ceased to bleed are filled with blood clots. This suggests that the clotting of blood has stopped the haemorrhage. However, there is a tendency for patients to bleed for long periods from even slight injuries in conditions with defective blood clotting [2]. For example, trauma is the fourth-leading cause of death in the United States for all ages, and many, if not most, civilian trauma deaths are due to haemorrhagic shock [3, 4]. In addition, although blood coagulation is vital to the preservation of life, blood clots can impede blood flows in vessels. Thrombus formation is responsible for most heart attacks and strokes and complicates other pathological conditions, coronary thrombosis, peripheral deep venous thrombosis, and pulmonary embolus, for example. It can eventually cause death unless brought under control [5]. A powerful technique for the investigation of both mechanism and blood coagulation process will be mostly helpful in clinic diagnosis.

Previous studies on blood coagulation detection methods include thrombelastography [6], ultrasound [5], transient elastography [7], quartz chemical analyser [8], optical coherence tomography (OCT) [9], etc. Hanke et al. [6] studied the impairment of whole blood coagulation and platelet function by hypertonic saline hydroxyethyl starch with rotation thrombelastometry. Huang et al. [5] investigated blood coagulation using ultrasound. Gennisson et al. [7] investigated the transient elastography method using a shear elasticity probe served to evaluate the shear wave velocity V_s and shear wave attenuation α_s of porcine whole blood during *in vitro* clot formation. The viscosity and elasticity detection methods used above have their own drawbacks because the measurement results depend on the quantity or viscosity of the fibrin and the strength of the magnetic element [9]. The turbidity detection method avoids the shortcoming of the viscosity detection, because it takes advantage of the transmitted light or the scattered light detection method [9]. OCT is an advanced high-resolution structural imaging technique which measures the intensity of back-reflected near-IR light. With this technique it is possible to perform noninvasive cross-sectional imaging of internal structures in biological tissues [10]. OCT has demonstrated considerable potential for static and dynamic imaging of various kinds of tissue and blood. OCT has the major advantage of providing a description of blood properties with high resolution, high sensitivity. Recently, the blood properties have been widely studied using OCT and optical Doppler tomography (ODT) due to their high resolution, real time, and noninvasive capabilities [11]. For example, previous studies have investigated the feasibility of OCT to provide a description of the coagulation process [12–14].

Fluid resuscitation has been a long standing therapy for trauma and hemorrhagic shock to restore blood volume, cardiac output and flow to the microcirculation. Lactated Ringer's and Hextend are the primary fluids used by many trauma unites and the US Army for pre-hospital resuscitation [15–21]. Some advancing level of haemodilution logically must diminish the ability of blood to coagulate [22]. As shown in a previous study, 7.5% hypertonic saline solution has anticoagulant effects when it replaces 7.5% or more of blood vol-

B. Liu, Y. Liu, H. Wei, X. Yang, Z. Guo MOE Key Laboratory of Laser Life Science & Institute of Laser Life Science, College of Biophotonics, South China Normal University, Guangzhou 510631, Guangdong Province, China; e-mail: weihj@scnu.edu.cn;
G. Wu Department of Surgery, the First Affiliated Hospital, Sun Yat-Sen University, Guangzhou 510080, Guangdong Province, China;
H. Yang, S. Xie Key Laboratory of Optoelectronic Science and Technology for Medicine of Ministry of Education of China, Fujian Normal University, Fuzhou 350007, Fujian, China;
Y. He Graduate School at Shenzhen, Tsinghua University, Shenzhen 518055, Guangdong, China

Received 22 July 2016; revision received 30 September 2016
Kvantovaya Elektronika **46** (11) 1055–1060 (2016)
Submitted in English

ume [23]. Conversely, the addition of either normal saline or Haemaccel to a 20% dilution *in vitro* renders blood hypercoagulable [24]. Recently, the effects of *in vitro* dilution of blood with various solutions on blood coagulation have been investigated. Sutton [25] studied the effect of digitalis on coagulation of blood in 1950. Strauss et al. [26] studied the effects of hydroxyethyl starch on fibrinogen, fibrin clot formation and fibrinolysis. Egli et al. [27] compared the effects of progressive *in vitro* haemodilution with hydroxyethyl starch, gelatin and albumin with haemodilution using 0.9% saline in patients. Wade et al. [3] investigated the efficiency of hypertonic 7.5% saline and 6% dextran-70 in treating trauma. Luostarinen et al. [28] made a comparison of hypertonic saline and mannitol on whole blood coagulation *in vitro*.

The purpose of this study is to investigate the effects of hypertonic (7.5%) and normal saline (0.9%) on the coagulation process using OCT and to demonstrate the capability of the OCT technique for quantifying the light penetration depth $D_{1/e}$ and attenuation coefficient α_s of diluted blood by an *in vitro* assessment.

2. Materials and methods

2.1. Experimental setup

In this study, a spectral domain OCT system (SD-OCT) (Shenzhen MOPTIM Imaging Technique Co., Ltd., China) [29] was used for the measurement. A schematic of the OCT system was shown in paper [30]. A low-coherence broadband superluminescent diode with a centre wavelength of 830 ± 40 nm was used as the optical source. The output power of the optical source was 5 mW. The axial and transverse resolutions of the OCT system were about 15 and 25 μm in free space, respectively, which were determined by the focal spot size of the probe beam. The signal-to-noise ratio was 120 dB in this system and the lateral and in-depth scanning was 3 and 1.8 mm, respectively. Two-dimensional (2D) images were obtained through scanning the incident beam over the sample surface in the lateral direction and in-depth (A-scan) scanning by the interferometer. The acquisition time per OCT image was 180 ms, which corresponds to an A-scan frequency of 2000 Hz. A personal computer was used to control the OCT system. The data acquisition software was written in Lab View 7.2-D. 2D OCT images obtained in the experiment were stored in the personal computer for further processing.

2.2. Materials

The experimental protocol was approved by the Affiliated Hospital of Sun Yat-sen University. The experiment was performed on 12 healthy young volunteers (6 men and 6 women) aged from 23 to 30. A signed informed consent was obtained from each subject before the experiment.

Blood sampling was performed only once a day in each volunteer at 9 a.m. after an overnight fast. Blood was drawn from an antecubital vein through a 25-gauge butterfly needle. About 2 mL of blood was then collected into vacuum-drying test tubes containing no anticoagulants. Prepared 0.9% normal saline and 7.5% hypertonic saline were added to the whole blood samples. The percentage replacement of blood by normal or hypertonic saline was as follows:

1) 0.9% normal saline 0.04 mL (2% blood volume) with 1.96 mL whole blood;

2) 7.5% hypertonic saline 0.04 mL (2% blood volume) with 1.96 mL whole blood;

3) 0.9% normal saline 0.22 mL (111056% blood volume) with 1.78 mL whole blood;

4) 7.5% hypertonic saline 0.22 mL (11% blood volume) with 1.78 mL whole blood;

5) 0.9% normal saline 0.4 mL (20% blood volume) with 1.6 mL whole blood;

6) 7.5% hypertonic saline 0.4 mL (20% blood volume) with 1.6 mL whole blood.

Each freshly acquired blood sample with no additional processing was immediately monitored with OCT for 1 hour to obtain the one-dimensional (1D) diagrams of optical intensity versus depth. This means that each coagulation process occurred spontaneously. Normal whole blood served as the control group.

2.3. OCT measurements

A round glassware of about 10 mm in height and 20 mm in diameter was used as a blood sample container. The sample container was placed on the pedestal almost perpendicular to the probe beam. Each freshly acquired 2 mL of blood was tiled to cover the base of the blood sample container with a pipette. The measurements were immediately performed with 2D OCT functional imaging (0 min) and then OCT images were taken every 30 s within 60 min after sampling. The room temperature was maintained at 22 °C throughout the experiments. 2D OCT images obtained in each experiment were stored in the computer for further processing.

2.4. Methods

A 1D averaged optical intensity profile that represents the in-depth reflected light intensity distribution was obtained by averaging the 2D image laterally [31]. The penetration depth $D_{1/e}$ was obtained by applying a best fit exponential curve in depth to the averaged and normalised signal intensity data [14, 32, 33].

The clinical value of OCT depends on high imaging speed to provide real time in vivo imaging, high spatial resolution to resolve small tissue structures and sufficient contrast to discriminate between those structures [34]. Contrast in OCT images originates from differences in reflectivity of different tissues, which are caused by their variation in the refractive index n. Unfortunately, contrast is limited because for most tissue n only ranges from 1.3 to 1.4 [34]. Measurement of the attenuation coefficient can provide additional information and may increase the clinical potential of OCT by allowing quantitative discrimination between different tissue types [34].

Tissue optical properties can be determined with OCT by fitting a model to the OCT signal. Two models have been frequently used for the description of OCT signal: the single-scattering model and the multiple-scattering model [35–41]. A previous study has shown that, with a proper correction for the confocal properties of the sample arm, both models are appropriate to extract the scattering coefficients of weakly scattering media. However, for high scattering media, the multiple scattering should be taken into account, and the multiple-scattering model can provide higher accuracy [37]. In this study, whole blood is a highly scattering and absorbing medium in the visible and near-IR region [42]. The optical attenuation coefficient of blood can be quantified from the

intensity of the detected light versus the depth. The reflected light intensity depends on blood's optical property, i.e., the absorption coefficient μ_a and scattering coefficient μ_s, or total attenuation coefficient μ_t: $\mu_t = \mu_s + \mu_a$ [43]. These physical properties play a vital role in the assessment of tissue features, which are unique to the biological tissue [30, 39, 44, 45]. In this study, the measured signal is defined as [39, 40, 45]:

$$[\langle i^2(z)\rangle]^{1/2} \approx (\langle i^2\rangle_0]^{1/2}[\exp(-2\mu_t z)]^{1/2}, \quad (1)$$

where $\langle i^2(z)\rangle$ is the photodetector heterodyne signal current received by the OCT system from the probing depth z and $\langle i^2\rangle_0$ is the mean square heterodyne signal. The result of the OCT study is the measurement of optical backscattering or reflectance $R(z) \propto [\langle i^2(z)\rangle]^{1/2}$ from blood versus axial ranging distance, or depth, z. Thus, it follows that the reflected power can be approximately proportional to $-\mu_t z$ in exponential scale according to the single scattering model:

$$R(z) \propto [\langle i^2(z)\rangle]^{1/2} = I_0 a(z)\exp(-\mu_t z), \quad (2)$$

where I_0 is the incident light intensity launched into the blood sample and $a(z)$ is the reflectivity of blood at depth z. Therefore, measurement of OCT reflectance for depth z_1 and z_2 allows for approximate evaluation of the attenuation coefficient and its temporal behaviour. The coefficient μ_t can be obtained theoretically from the reflectance measurements at two different depths, z_1 and z_2 [39, 40, 45]:

$$\mu_t = \frac{1}{\Delta z}\ln\left[\frac{R(z_1)}{R(z_2)}\right], \quad (3)$$

where $\Delta z = |z_1 - z_2|$. As noise is inevitable in the measurement, the final result should be obtained by the use of a least-square fitting method in order to improve the accuracy of determining μ_t. An averaged intensity profile as a function of depth was obtained by averaging the 2D images laterally over approximately 1 mm, which was enough for speckle noise suppression. A best-fit exponential curve was applied to the averaged intensity profiles of each group since the noise is unavoidable in the measurement.

2.5. Statistical analysis

All data from all samples were presented as a 'mean ± standard deviation' and analysed by a Student's t-test. All statistical analyses were performed with the statistics software SPSS 10.0 for Windows. The value $p < 0.05$ indicated a significant difference.

3. Results and discussion

OCT is based on low-coherence interferometry to produce cross-sectional tomographic imaging of the microstructure in biological tissues by measuring the magnitude of backscattered light [46]. One main advantage of this technique is the ability to investigate turbid and highly scattering media, such as biological tissues and whole blood. Whole blood is a highly scattering and absorbing medium in the visible and near infrared region. Erythrocytes [red blood cells (RBCs)] are the main scattering elements in blood. The scattering properties of erythrocytes are determined by shape, size, volume and mass. The optical properties also depend on the concentration of haemoglobin (Hb) in the erythrocyte. Scattering properties of blood mainly depend on haematocrit, which is the volume fraction of RBCs [47]. Other effects which influence scattering properties of blood are sedimentation and aggregation of RBCs, as well as coagulation and deformation of cells [48].

As can be seen from the 1D averaged optical intensity profile that represents the in-depth reflected light intensity distribution, the boundary between blood plasma and the RBC layer moves with time. This movement defines the sedimentation rate of blood [12]. Normal blood sedimentation might cause a problem for accurate measurements of blood coagulation. Thanks to the slight sedimentation property of blood during coagulation, we could accurately calculate $D_{1/e}$ and μ_t of the blood samples from the OCT in-depth reflectance profiles with the methods mentioned above [4].

Figure 1 illustrates the variations in average $D_{1/e}$ as a function of time acquired from normal whole blood, whole blood diluted with 0.9% normal saline and blood diluted with 7.5% hypertonic saline. During coagulation, the fibrinogen in the plasma transforms to coarse fibrin. The formation of fibrin leads to an increase in the refractive index of the plasma, which results in a decrease in the refractive index mismatching between the red blood cells and the plasma.

It leads to a decrease in blood scattering and, as a result, to the enhancement of $D_{1/e}$ and a decrease in the attenuation coefficient. The variation in $D_{1/e}$ for each group is represented by a convex curve characterized by two stages. The first stage of each group corresponds to a rapid increase in the penetration depth, and the second stage corresponds to a very slow increase. The curves of the variations in $D_{1/e}$ can be linked to changes in the state of the medium and coincide with the two stages of a liquid to a solid–gel state [49]. At the initial moment, the medium was in a liquid state. During the first stage, the medium turned into a gel state as a result of the transformation of fibrinogen into fibrin [14].

In this stage, $D_{1/e}$ increased rapidly. The second stage coincides with the solid–gel state of the medium. To better characterise variations in blood properties during coagulation, the coagulation time t_c is defined as the period of time where $D_{1/e}$ curve is saturated with the time elapsed. One can see from Fig. 1 that for blood samples with blood volume replacement of 2%, 11% and 20% by 0.9% normal saline the average coagulation times t_c are 420 ± 16, 418 ± 16 and 358 ± 14 s (as indicated by arrows in Fig. 1), respectively. For blood samples with blood volume replacement of 2%, 11% and 20% by 7.5% hypertonic saline t_c are equal to 422 ± 17, 1160 ± 45 and 1730 ± 69 s (as indicated by arrows in Fig. 1), respectively. The average coagulation time for normal whole blood is 425 ± 19 s.

Figure 2 shows the time dependences of the average attenuation coefficients in normal whole blood, whole blood diluted with 0.9% normal saline and whole blood diluted with 7.5% hypertonic saline. One can see that the attenuation coefficients decrease slowly within 60 min by about 2.6%, 2.3% and 1.4%, respectively, for blood samples with blood volume replacement of 2%, 11% and 20% by 0.9% normal saline. The total decrease in the attenuation coefficient for blood samples with blood volume replacement of 2%, 11% and 20% by 7.5% hypertonic saline is 2.7%, 3.8%, and 6.1%, respectively. The average attenuation coefficient decreases by 2.5% for the control group.

With replacement of 11% blood volume or less by 0.9% normal saline and 2% blood volume by 7.5% hypertonic saline, there were no significant differences in $D_{1/e}$ or the

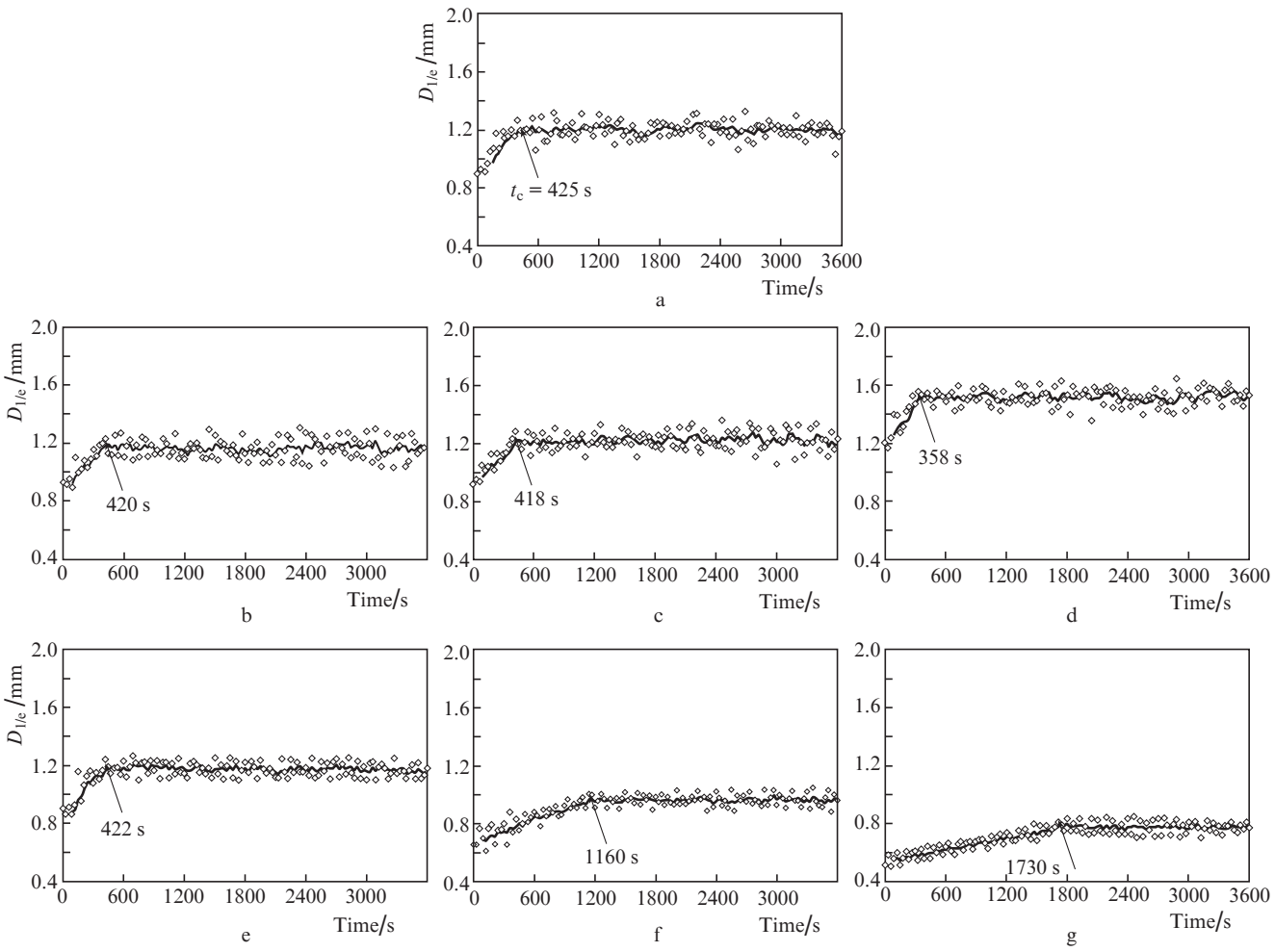

Figure 1. Evolution of average light penetration depth $D_{1/e}$ as a function of time during 60-min blood coagulation for (a) normal whole blood, whole blood with blood volume replacement of (b) 2%, (c) 11% and (d) 20% by 0.9% normal saline, and those with blood volume replacement of (e) 2%, (f) 11% and (g) 20% by 7.5% hypertonic saline.

attenuation coefficient compared with the control group. With replacement of 11% blood volume or more by 7.5% hypertonic saline and 20% blood volume by 0.9% normal saline, $D_{1/e}$ and the attenuation coefficient were apparently different from the control group.

4. Conclusions

Although the intuitive assumption is that haemodilution would increase bleeding tendencies through dilution of coagulation factors, in reality, the reserve capacity of the coagulation system under normal conditions is so great that dilution is of no relevance unless large volumes are used [24]. Dilution with different solutions may have different effects on blood coagulation process.

In this paper, measurements of $D_{1/e}$ and μ_t permit description of the dynamics of the blood coagulation process. The value of t_c makes it possible to describe two successive stages of the blood coagulation process. With replacement of 20% blood volume by 0.9% normal saline, t_c is apparently shorter compared with the control group. On the contrary, t_c is much longer than that in the control group when 11% blood volume or more were replaced by 7.5% hypertonic saline. These results indicate that there is a procoagulant effect up to a dilution of 20% with 0.9% normal saline. There is an anticoagulant effect up to a dilution of 11% or more with 7.5% hypertonic saline.

These results are consistent with previous studies [23, 24]. It is concluded that OCT is a potential technique to quantify and control the liquid–gel transition of blood diluted by normal and hypertonic saline during coagulation. Our study may be helpful in clinical therapy, preventing vast blood bleeding in emergency, for example. However, treatment of haemorrhage with isotonic fluids such as normal saline is often inadequate because of the large volumes required, the short transport times in which to administer the fluids, and the use of small-bore peripheral venous cannulas [3]. Treatment with 7.5% hypertonic saline may be of benefit for patients. Our future studies will focus on investigating the influence of 7.5% hypertonic saline combined with different agents on blood coagulation with OCT.

Acknowledgements. This work was supported by the National Natural Science Foundation of China (Grant Nos 60778047, 61335011, 61275187 and 81071790), Specialised Research Fund for the Doctoral Programme of Higher Education of China (Grant Nos 20114407110001 and 200805740003), the Science and Technology Innovation Project of the Education Department of Guangdong Province of China, the Natural Science Foundation of Guangdong Province of China (Grant

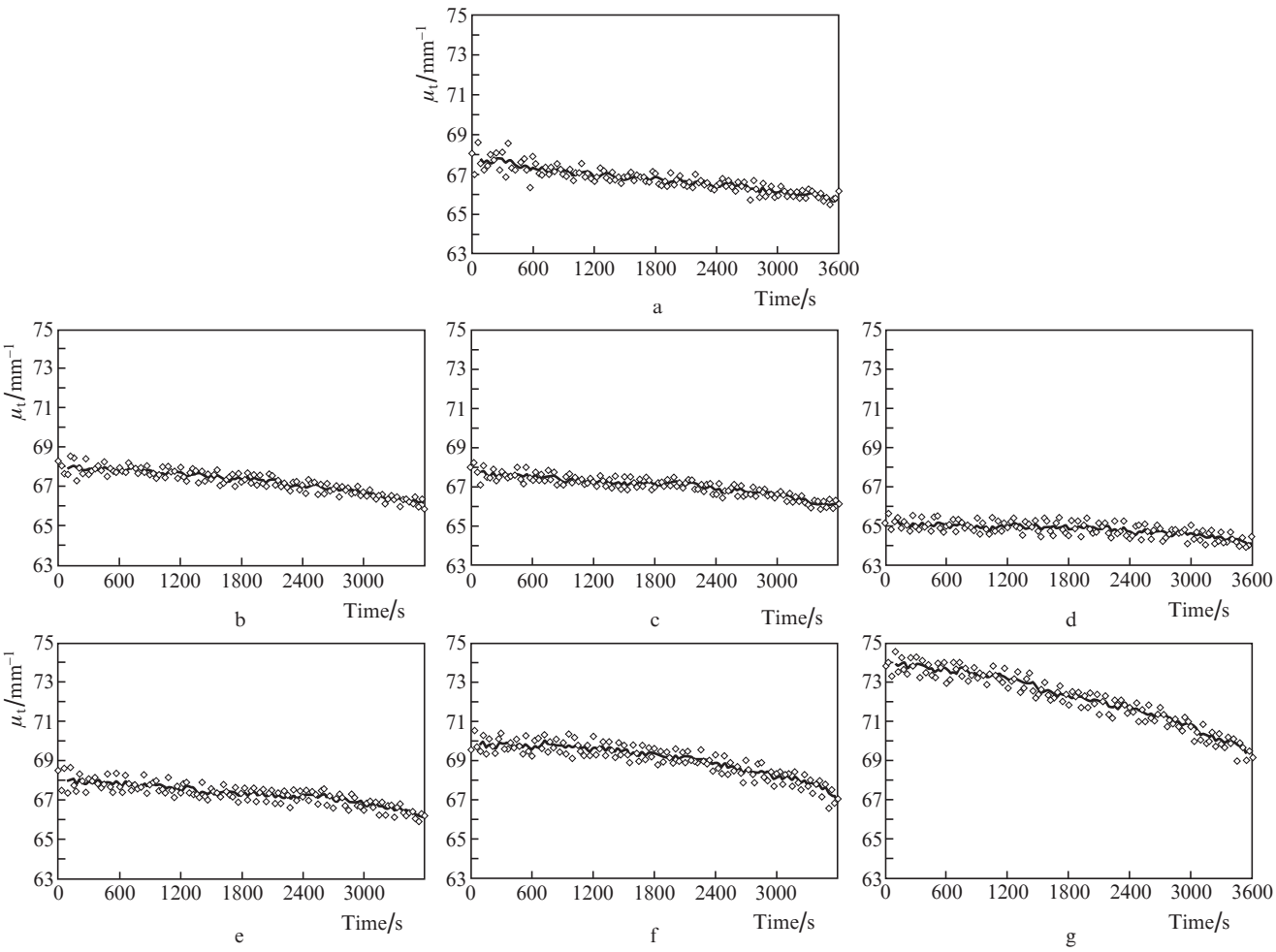

Figure 2. Evolution of the average attenuation coefficient as a function of time during the 60-min blood coagulation for (a) normal whole blood, whole blood with blood volume replacement of (b) 2%, (c) 11% and (d) 20% by 0.9% normal saline, and those with blood volume replacement of (e) 2%, (f) 11% and (g) 20% by 7.5% hypertonic saline.

Nos 06025080 and 9251063101000009), Technique Invention Programme of Guangdong Province (2013KJCX0052), the Science and Technology Project of Guangdong Province (2012A080203008), and Key Laboratory of Optoelectronic Science and Technology for Medicine (Fujian Normal University), Ministry of Education, China (Grant No. JYG1202).

References

1. Furie B., Furie B.C. *Cell*, **53**, 505 (1988).
2. Macfarlane R.G. *J. Clin. Pathol*., **1**, 113 (1948).
3. Wade C.E., Kramer G.C., Grady J.J., Fabian T.C., Younes R.N. *Surgery*, **122**, 609 (1997).
4. Mackenzie E.J., Morris J.A., Smith G.S., Fahey M. *J. Trauma*, **30**, 1096 (1990).
5. Huang C.C., Lin Y.H., Liu T.Y., Lee P.Y., Wang S.H. *J. Med. Biol. Eng*., **31**, 79 (2011).
6. Hanke A.A., Maschler S., Schöchl H., Flöricke F., Görlinger K., Zanger K., Kienbaum P. *Scand. J. Trauma Resusc. Emerg. Med*., **19**, 12 (2011).
7. Gennisson J.L., Lerouge S., Cloutier G. *Ultrasound Med. Biol*., **32**, 1529 (2006).
8. Muramatsu H., Kimura K., Ataka T., Homma R., Miyra Y., Karube I. *Biosens. Bioelectron*., **6**, 353 (1991).
9. Xu X.Q., Lin J. *Proc. SPIE Int. Opt. Soc. Eng*., **7845**, 784508 (2010).
10. Huang D., Swanson E.A., Lin C.P., Schuman J.S., Stinson W.G., Chang W., Hee M.R., Flotte T., Gregory K., Puliafito C.A., Fujimoto J.G. *Science*, **254**, 1178 (1991).
11. Xu X.Q., Geng J.H., Liu G.J., Chen Z.P. *IEEE T. Biomed. Eng*., **60**, 2100 (2013).
12. Tuchin V.V., Xu X., Wang R.K. *Appl. Opt*., **41**, 258 (2002).
13. Popescu D.P., Sowa M.G. *Phys. Med. Biol*., **54**, 4759 (2009).
14. Xu X.Q., Lin J., Fu F.F. *J. Biomed. Opt*., **16**, 096002 (2011).
15. Darlington D.N., Kremenevskiy I., Pusateri A.E., Scherer M.R., Fedyk C.G., Kheirabaldi B.S., Delgado A.V., Dubick M.A. *Int. J. Burn Trauma*, **2**, 42 (2012).
16. Dailey S.E., Dysart C.B., Langan D.R., Slye M.J., Nuttall G.A., Schrader L.M., Williams B.A., Oliver W.C. *J. Cardiothor. Vasc. An*., **19**, 358 (2005).
17. Handrigan M.T., Bentley T.B., Oliver J.D., Tabaku L.S., Burge J.R., Atkins J.L. *Shock*, **23**, 337 (2005).
18. Rafie A.D., Rath P.A., Michell M.W., Kirschner R.A., Deyo D.J., Prough D.S., Grady J.J., Kramer G.C. *Shock*, **22**, 262 (2004).
19. Sapsford W., Watts S., Cooper G., Kirkman E. *J. Trauma*, **62**, 868 (2007).
20. Spinella P.C., Perkins J.G., McLaughlin D.F., Niles S.E., Grathwohl K.W., Beekley A.C., Salinas J., Mehta S., Wade C.E., Holcomb J.B. *J. Trauma*, **64**, 286 (2008).
21. Todd S.R., Malinoski D., Muller P.J., Schreiber M.A. *J. Trauma*, **59**, 589 (2005).
22. Tobias M.D., Wambold D., Pilla M.A., Greer F. *J. Clin. Anesth*., **10**, 366 (1998).
23. Tan T.S., Tan K.H.S., Ng H.P., Loh M.W. *Anaesthesia*, **57**, 644 (2002).

24. Ruttmann T.G., James M.F.M., Viljoen J.F. *Brit. J. Anaesth*., **76**, 412 (1996).
25. Sutton G.C. *Circulation*, **2**, 271 (1950).
26. Strauss R.G., Stump D.C., Henriksen R.A., Saunders R. *Transfusion*, **25**, 230 (1985).
27. Egli G.A., Zollinger A., Seifert B., Pasch T., Spahn D.R. *J. Anaesth*., **78**, 684 (1997).
28. Luostarinen T., Niiya T., Schramko A., Rosenberg P., Niemi T. *Neurocrit. Care*, **14**, 238 (2011).
29. Wei H.J., Wu G.Y., Guo Z.Y., Yang H.Q., He Y.H., Xie S.S., Guo X. *J. Biomed. Opt*., **17**, 116006 (2012).
30. Zhao Q., Zhou C., Wei H., He Y., Chai X., Ren Q. *J. Biomed. Opt*., **17**, 105004 (2012).
31. Zhu Z.G., Wei H.J., Wu G.Y., Yang H.Q., He Y.H., Xie S.S. *J. Biomed. Opt*., **17**, 086002 (2012).
32. Xu X., Zhu Q. *IEEE J. Sel. Top. Quantum Electron*., **14**, 56 (2008).
33. Xu X., Zhu Q., Sun C. *IEEE Photonic. Tech. L*., **20**, 2117 (2008).
34. Faber D.J., van der Meer F.J., Aalders M.C.G. *Opt. Express*, **12**, 4353 (2004).
35. Schmitt J.M., Knüttel A., Bonner R.F. *Appl. Opt*., **32**, 6032 (1993).
36. Van der Meer F.J., Faber D.J., Sassoon D.M.B., Aalders M.C., Pasterkamp G., van Leeuwen T.G. *IEEE Trans. Med. Imaging*, **24**, 1369 (2005).
37. Lee P., Gao W.R., Zhang X.L. *Appl. Opt*., **49**, 3538 (2010).
38. Schmitt J.M., Knüttel A. *J. Opt. Soc. Am. A*, **14**, 1231 (1997).
39. Levitz D., Thrane L., Frosz M.H., Andersen P.E., Andersen C.B., Valanciunaite J., Swartling J., Anderson-Engels S., Hansen P.R. *Opt. Express*, **12**, 249 (2004).
40. Thrane L., Yura H.T., Andersen P.E. *J. Opt. Soc. Am. A*, **17**, 484 (2000).
41. Van Soest G., Goderie T., Regar E., Koljenović S., van Leenders G.L.J.H., Gonzalo N., van Noorden S., Okamura T., Bouma B.E., Tearney G.J., Oosterhuis J.W., Serruys P.W., van der Steen A.F.W. *J. Biomed. Opt*., **15**, 011105 (2010).
42. Zhernovaya O., Tuchin V.V., Leahy M.J. *J. Biomed. Opt*., **18**, 026014 (2013).
43. Xu X.Q., Wang R.K., Elder J.B., Tuchin V.V. *Phys. Med. Biol*., **48**, 1205 (2003).
44. Kodach V.M., Faber D.J., van Marle J., van Leeuwen T.G., Kalkman J. *Opt. Express*, **19**, 6131 (2011).
45. Yang Y., Wang T.H., Biswal N.C., Wang X.H., Sanders M., Brewer M., Zhu Q. *J. Biomed. Opt*., **16**, 090504 (2011).
46. Kirillin M.Yu., Meglinski I.V., Priezzhev A.V. *Quantum Electron*., **36**, 247 (2006).
47. Yaroslavsky A.N., Priezzhev A.V., Rodrigues J., Yaroslavsky I.V., Battarbee H., in *Handbook of Optical Biomedical Diagnostics.* Ed. by V.V. Tuchin (SPIE Press, 2002) Chap. 2.
48. Zhernovaya O., Tuchin V.V., Leahya M.J. *J. Biomed. Opt*., **18**, 026014 (2013).
49. Reed R.L., Johnston T.D., Chen Y., Fischer R.P. *J. Trauma*, **31**, 8 (1991).